Desalination and Water Treatment
www.deswater.com

doi: 10.1080/19443994.2016.1184188

57 (2016) 28133–28140
December

Taylor & Francis
Taylor & Francis Group

Improvement of vertically aligned carbon nanotube membranes: desalination potential, flux enhancement and scale-up

Youngbin Baek[a,e], Dong Kyun Seo[b], Jong Ho Choi[b], Byeongho Lee[a], Yong Hyup Kim[b], Seung Min Park[c], Jungwoo Jung[c], Sangho Lee[c], Jeyong Yoon[a,d,*]

[a]*School of Chemical and Biological Engineering, Institute of Chemical Process, Seoul National University (SNU), Daehak-dong, Gwanak-gu, Seoul 08826, Republic of Korea, Tel. +1 814 826 5172; email: ykb5033@psu.edu (Y. Baek), Tel. +82 2 880 8941; email: bhlee79@snu.ac.kr (B. Lee), Tel. +82 2 880 8927; Fax: +82 2 876 8911; email: jeyong@snu.ac.kr (J. Yoon)*
[b]*School of Mechanical and Aerospace Engineering, Seoul National University, Daehak-dong, Gwanak-gu, Seoul 08826, Republic of Korea, Tel. +82 2 880 1728; emails: crew101@snu.ac.kr (D.K. Seo), followjongho@snu.ac.kr (J.H. Choi), yongkim@snu.ac.kr (Y.H. Kim)*
[c]*Department of Civil and Environment Engineering, Kookmin University, Jeongneung-gil 77, Seongbuk-gu, Seoul 02707, Republic of Korea, Tel. +82 2 910 5060; emails: baentac@gmail.com (S.M. Park), sawoo21@daum.net (J. Jung), Tel. +82 2 910 4529; Fax: +82 2 910 8597; email: sanghlee@kookmin.ac.kr (S. Lee)*
[d]*Asian Insititute for Energy, Environment & Sustainability(AIEES), Seoul National University, Daehak-dong, Gwanak-gu, Seoul 08826, Republic of Korea*
[e]*Department of Chemical Engineering, The Pennsylvania State University, University Park, PA 16802, United States*

Received 17 February 2016; Accepted 24 April 2016

ABSTRACT

Carbon nanotube (CNT) membranes are considered as next-generation membranes for desalination. Among the various types of CNT membranes, vertically aligned (VA) CNT membranes provide rapid water transport. However, when the water permeability of VA CNT membranes are compared with those of the commercial membrane, the VA CNT membranes only showed slightly higher water permeability due to their low pore densities. Additionally, the applicability of VA CNT membranes for desalination has been limited due to their larger pore sizes. Herein, we improved VA CNT membranes in terms of the desalination potential, flux enhancement, and scale-up. For the desalination potential, graphene oxide (GO) or polyamide (PA) were coated on a VA CNT membrane as a selective layer, which showed approximately 40–65% NaCl rejection, respectively. A pretreatment polyelectrolyte coating for a GO-coated VA CNT membrane increased the water permeability by approximately 50%. For the flux enhancement, the water permeability of a VA CNT membrane was nearly doubled when the VA CNT forest was mechanically densified by half. Finally, an enlarged VA CNT forest (2×2 cm^2), sequential VA CNT forests (1×1 cm^2) in a large cast, and an assembly of the VA CNT membrane were suggested as scale-up approaches.

Keywords: Carbon nanotube (CNT) membrane; Vertically aligned CNT; Desalination; Flux enhancement; Scale-up

*Corresponding author.

1. Introduction

Carbon nanotube (CNT) membranes have been considered as one of the next-generation desalination membranes [1,2]. CNT membranes are known to be high performance and/or fouling-resistant membranes due to their unique properties, such as rapid transport of water molecules [3] and antimicrobial properties [4]. Currently developed CNT membranes can be classified as vertically aligned (VA) CNT membranes or mixed CNT membranes. VA CNT membranes can be fabricated using an as-grown VA CNT forest itself or adding filler encapsulation in VA CNT forest. On the other hand, mixed CNT membranes can be fabricated by inserting modified CNTs during the polymerization process (i.e. phase inversion for UF and interfacial polymerization for NF/RO) [5].

VA CNT membrane composites typically utilize an inner wall or an outer wall of CNTs as a pore. These membranes usually show much higher water permeability than mixed CNT membranes. Water transport through a CNT wall is tens of thousands times faster than conventional water transport due to the hydrophobic surface properties of the CNT wall [6]. According to previous studies, this enhancement factor ranged from 3,000 to 61,000, depending on the use of a double-wall CNT (DWNT) or multi-wall CNT (MWNT) [7,8]. Note that the enhancement factor indicates the extent of the increased flux, which is expressed as the measured flux over the calculated flux by the Hagen–Poiseuille equation. Despite this fast water transport through CNTs, we previously reported that a VA CNT membrane had only 2–3 times enhanced water flux than a commercial UF membrane due to a smaller pore size, lower pore density, and greater thickness [9].

Additionally, VA CNT membranes are not typically used for desalination. According to a simulation study, a 0.59 nm inner diameter CNT showed 95% of salt rejection, and a 0.75 nm inner diameter CNT decreased salt rejection to 58% [10]. This indicated that the inner diameter of CNTs should be < 0.6 nm for desalination, which is limited in current technology. Furthermore, CNTs with sub-2 nm pore sizes showed about 0% salt rejection of a 10 mM KCl solution [11]. Other studies have attempted to increase the desalination potential of VA CNT membranes. For example, a "gate-keeper" has been functionalized onto CNTs to enhance ion selectivity [12]. The smallest pore size of these functionalized VA CNT membranes was 3.3 nm, which was larger than most mono-and di-valent ions. Another attempt polymerized VA CNT membranes by using a grafting technique, but showed no Na_2SO_4 rejection [13].

In this work, we improved the desalination potential and flux properties of VA CNT membranes and further suggested scale-up approaches. First, graphene oxide (GO) or polyamide (PA) was coated onto a VA CNT membrane as a selective ion-separating layer. Second, the VA CNT forest was mechanically densified to enhance water permeability by increasing the pore density. Finally, three scale-up approaches were suggested.

2. Materials and methods

2.1. Fabrication of VA CNT membranes

VA CNT membranes were fabricated as follows. CNTs were vertically grown by water-assisted thermal chemical vapor deposition method [14,15]. VA CNTs were filled up with epoxy resin (Epon 828, Miller–stephenson Inc., CA) under about 0.1 bar of vacuum condition. After the epoxy-VA CNTs matrix was hardened, pores were formed through cutting the matrix using an ultramicrotome (HM 340 E, MICROM Lab., Germany). More details about VA CNTs and VA CNT membranes are described in our previous study [9].

2.2. Active layer coating on the VA CNT membrane for desalination

2.2.1. Graphene oxide (GO) coating

GO platelets were synthesized from graphite (Bay Carbon, SP-1, USA) using the modified Hummers method [16]. A solution mixture of graphite powder, sulfuric acid (>98%, Sigma-Aldrich, USA), and potassium permanganate (>99%, Sigma-Aldrich, USA) in a beaker was stirred for 6 h at 45˚C. The solution was neutralized by deionized (DI) water (Barnsted NANO Pure, USA) with hydrogen peroxide (>30%, Sigma-Aldrich, USA). The brown-colored solution was rinsed with DI water in triplicate to completely remove any residual acid and salt in the solution. The GO powders were obtained by filtering the solution using a polytetrafluoroethylene (PTFE) membrane filter (47 mm diameter, 0.2 μm pore size, Whatman., Germany). After the GO powder was prepared, the GO platelets were re-dispersed in DI water with a concentration of 0.01 mg/mL and sonicated for 1 h to make a homogeneous suspension.

GO-coated VA CNT membrane was fabricated as follows. Polyallylamine hydrochloride (PAH; MW 65,000 g/mol, Sigma-Aldrich, USA) was used as buffering layer between the VA CNT membrane and the GO layer to avoid blocking pores directly through the deposition of the GO layer. 0.01 M PAH solution

was coated onto the VA CNT membrane using a spin-coater (ACE-200, Dong Ah Trade Corp., South Korea) [17]. A PAH solution was dropped on the VA CNT membrane and rotated for 20 s with 4,000 rpm of a rotation speed. Excess PAH was removed with DI water and the surface of the VA CNT membrane was dried by spinning for 20 s. After the dry process, 10 mL of 0.01 mg/mL GO solution was filtrated under vacuum on the approximately 0.1 cm^2 area of the VA CNT membrane.

2.2.2. Polyamide coating

Polyamide was synthesized onto the VA CNT membrane by interfacial polymerization. 3.0 wt.% of *m*-phenylenediamine (MPD, 99%, Sigma–Aldrich, USA) solution and 0.1 wt.% of trimesoyl chloride (TMC, 98%, Sigma–Aldrich, USA) solution were prepared in DI water and *n*-hexane (Samchun Chemicals, Korea), respectively. VA CNT membranes were immersed in MPD solution for 1 h and then, the excess MPD on the surface was removed by air knife. The TMC solution was poured on that surface for 1 min and washed by *n*-hexane after 1 min. This polyamide-coated VA CNT membrane was stored in the DI water before the measurement. Note that 3.0 wt.% of MPD solution was optimized in our previous study for CNT-embedded RO membrane because some MPD might be consumed by adsorption on the surface of CNTs while the polyamide RO membrane was synthesized with 2.0 wt.% of MPD solution [18].

2.3. Mechanical densification of VA CNT forest

VA CNT forest was mechanically densified to increase the pore density of the VA CNT membrane. After VA CNT forest was separated from the substrate, it was positioned on the Teflon cast to be compressed by applying mechanical force in the direction perpendicular to the CNT axis. The substrate area (A_0) was 2×1 cm^2, and those for the densified VA CNT forest (A_1) was 1×1 cm^2. Other processes were same as fabrication method for VA CNT membrane. This densification sufficiently increased the pore density of VA CNT membrane because it is difficult to control the CNT density during the CNT growth. More details for the mechanical densification are described in our previous study [19].

2.4. Membrane filtration test

Membrane performances (i.e. water permeability and salt rejection) were performed by the modified dead-end membrane filtration system [9,19]. The size of the VA CNT membrane was 1.3×1.3 cm^2. Pure water permeability of the surface-modified VA CNT

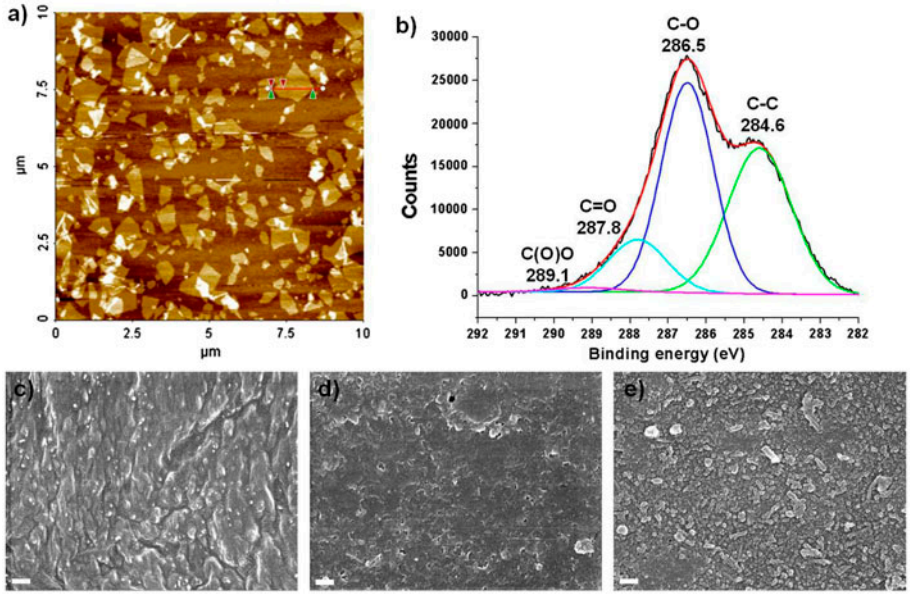

Fig. 1. Characteristics of graphene oxide (GO) platelets, GO-coated VA CNT membrane and polyamide (PA)-coated VA CNT membrane: (a) AFM image of the synthesized GO platelets, (b) XPS spectrum of the GO platelets, SEM images of the top surface in, (c) VA CNT membrane, (d) GO-coated VA CNT membrane, and (e) PA-coated VA CNT membrane (scale bar: 200 nm).

membrane was obtained by measuring the weight of the permeate for 5 min with DI water under 10 bar pressurized by N_2 gas. Water permeability and salt rejection were obtained with 10 mM NaCl solution in conditions of 15.5 bar of pressure, 600 rpm of stirring speed and room temperature. Water permeability (J_w) was calculated by $J_w = \Delta V/(a \times \Delta t \times P)$, where ΔV is the volume of the collected permeate, a is the effective area of the membrane, Δt is the measurement time, and P is the applied pressure. Rejection rate (R, %) was calculated by $R = (1 - C_p/C_f) \times 100\%$, where C_p is the salt concentration of the permeate and C_f is the salt concentration of the feed. The salt concentration was measured using a conductivity meter (Horiba, F-54 BW, Japan).

3. Results and discussion

3.1. Desalination potential of VA CNT membrane

3.1.1. Characteristics of GO platelets, GO-coated VA CNT membrane, and PA-coated VA CNT membrane

The characteristics of synthesized GO platelets and surface morphologies for GO-coated VA CNT membranes and PA-coated VA CNT membranes are illustrated in Fig. 1. The GO platelets mostly existed as monolayers ranging from a few hundred nm to a few μm (Fig. 1(a)). A C 1s XPS spectrum (Fig. 1(b)) showed peaks typical for GO platelets and indicative of a non-oxygenated carbon ring (284.6 eV) and C–O (286.5 eV), C=O (287.8 eV), and C–O–O (289.1 eV) bonds [20,21]. Surface morphologies for the VA CNT membranes were shown by SEM images (Fig. 1(c)–(e)). In Fig. 1(c), the white dots indicate the ends of the VA CNTs, i.e. the pores of the VA CNT membrane. After coating with GO, these dots disappeared under the GO layers (Fig. 1(d)). The surface morphology of the PA-coated VA CNT membrane showed a "ridge and valley" structure, which is typically observed in PA RO membranes (Fig. 1(e)) [22,23].

3.1.2. Water permeability and salt rejection

Fig. 2 shows the water permeability and the salt rejection for the GO-coated VA CNT membrane and the PA-coated VA CNT membrane. The pure water permeability for VA CNT membranes are shown in Fig. 2(a). The permeability of the GO-coated VA CNT membrane and the PA-coated VA CNT membrane decreased to 173 ± 27–187 ± 35 LMH bar^{-1}, respectively, which represented 83–84% decreases from that of a non-coated VA CNT membrane (1,100 ± 130 LMH bar^{-1}). This indicated that the GO and PA layers acted as dense active layers on the VA CNT membranes; these dense layers may impart some desalination ability.

To evaluate the desalination potential, the water permeability and the NaCl rejection of GO, 0.01 M PAH + GO and PA-coated VA CNT membranes were investigated using 10 mM NaCl solutions (Fig. 2(b)). The NaCl rejections for the GO, 0.01 M PAH + GO and PA-coated VA CNT membranes were 44.9 ± 7.6, 42.3 ± 6.1, and 64.8 ± 4.2%, respectively. However, the non-coated VA CNT membrane showed no NaCl rejection and had same water permeability as that under pure water conditions (Fig. 2(a)) due to a larger pore size (approximately 5 nm) [9]. GO layers have been shown to have some degree of NaCl rejection in previous studies. For example, ultrathin graphene

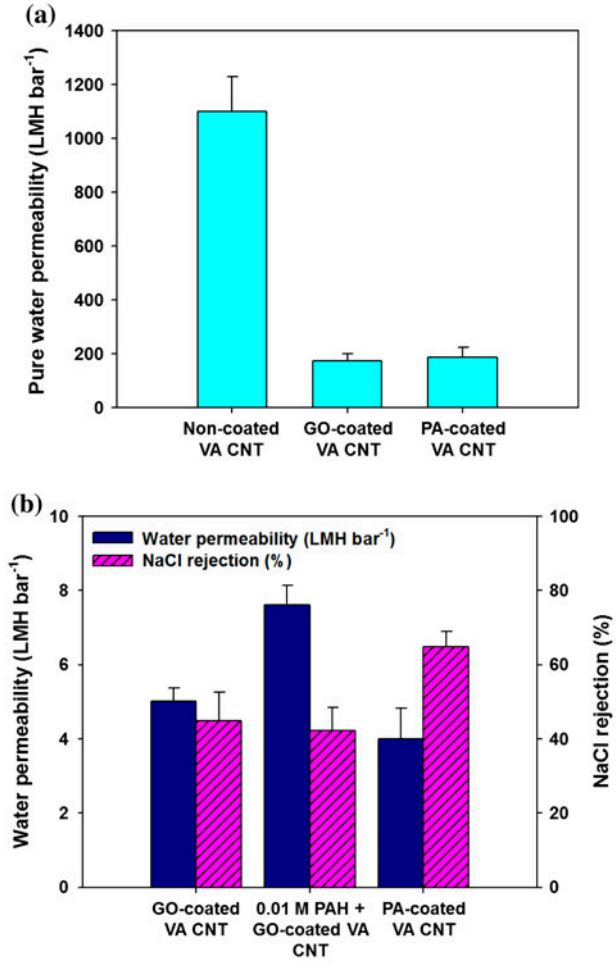

Fig. 2. Membrane performances: (a) pure water permeability of non-coated, GO-coated, and PA-coated VA CNT membranes and (b) water permeability and NaCl rejection of GO-coated, 0.01 M PAH + GO-coated, and PA-coated VA CNT membranes.

nanofiltration membranes showed 30–40% NaCl rejection [24,25]. This NaCl rejection property can be explained by the Donnan exclusion theory due to the negatively charged GO layer [26,27]. Because of an electrical repulsion force, Cl^- and Na^+ ions are both rejected to maintain solution electroneutrality. The narrow gap between GO layers could also account for this salt rejection property. The interlayer distance between GO sheets is approximately 0.7 nm [28], i.e. a size small enough to reject monovalent ion (the hydrated diameters of Na^+ ions and Cl^- ions are 0.716 and 0.664 nm, respectively [29]). The low NaCl rejections in this study can be explained by a high capillary force which helps the hydrated ions pass through the GO layers [30]. The PA-coated VA CNT membrane showed better rejection rates; however, these values were lower than those of commercial PA layers (>99%). The spiky surface morphology of the PA-coated VA CNT membranes could affect the formation of the PA (or GO) layer, and thereby affect the rejection rate. Furthermore, concentrations of the MPD and TMC monomers used in the preparation of the PA layer could have affected the VA CNT membrane. Overall, the GO and PA coating methods require further optimization to enhance VA CNT membrane desalination performances.

The water permeability of the GO, 0.01 M PAH + GO and PA-coated VA CNT membranes were 5.0 ± 0.4, 7.6 ± 0.5, and 4.0 ± 0.8 LMH bar^{-1}, respectively. The PAH treatment enhanced water permeability by 52% with only a 6% decrease in NaCl rejection, whereas the pure water permeability of the 0.01 M PAH-coated VA CNT membrane decreased to 75.8% (834 LMH bar^{-1}). The PAH coating acted as a bridge connecting the pores of the GO layers to the pores of the VA CNT membrane. The PA-coated VA CNT membrane had a water permeability of 4.0 ± 0.8 LMH bar^{-1} and a NaCl rejection of 64.8 ± 4.2%, i.e. a lower water permeability and a higher NaCl rejection than those of the GO-coated VA CNT membrane. The permeability of the PA layer was lower due to its dense structure. When compared with previous studies on the GO membranes, wherein 3.3 LMH bar^{-1} of water permeability and 40% NaCl rejection were reported [24,25], the performances of the GO, 0.01 M PAH + GO and PA-coated VA CNT membranes were slightly higher at 4.0–7.6 LMH bar^{-1} and 42–65%.

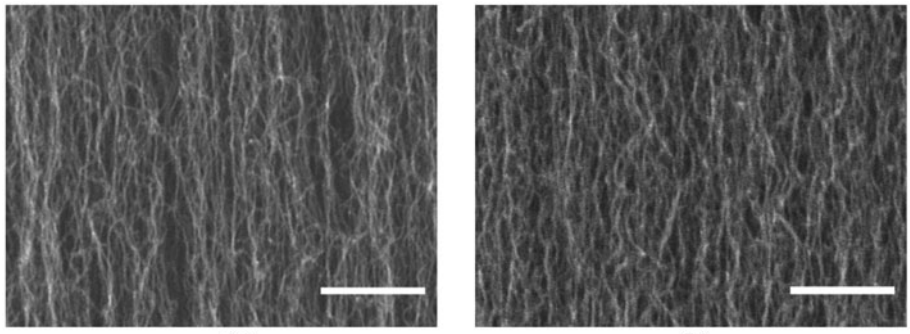

Fig. 3. Cross-sectional SEM images of (a) a pristine CNT forest and (b) a two times densified CNT forest (Scale bar: 500 nm).

Table 1
Water permeability for a pristine VA CNT membrane and a two times densified VA CNT membrane

	Pristine VA CNT membrane	Two times densified VA CNT membrane
CNT density[a] (#/cm^2)	6.8×10^{10}	1.3×10^{11}
Water permeability (LMH/bar)	1,100 ± 130	2,070 ± 260

[a]areal density of VA CNT forest was calculated by the geometric shape with following equation. Areal density of VA CNT $= \left(\frac{3\sqrt{3}a_{c-c}^2}{4\pi m_c N}\right) \cdot \left(\frac{M}{S\mathrm{L}\times \mathrm{d}_{outer}}\right)$; where a_{c-c} is the C–C bond length in a nanotube (0.144 nm), m_c is the mass of one carbon atom (1.993×10^{-20} mg), N is the average wall number, M is the mass of CNTs (mg), S is the CNT growth area (cm^2), L is the CNT height (cm), and d_{outer} is the outer-wall diameter (nm) [31].

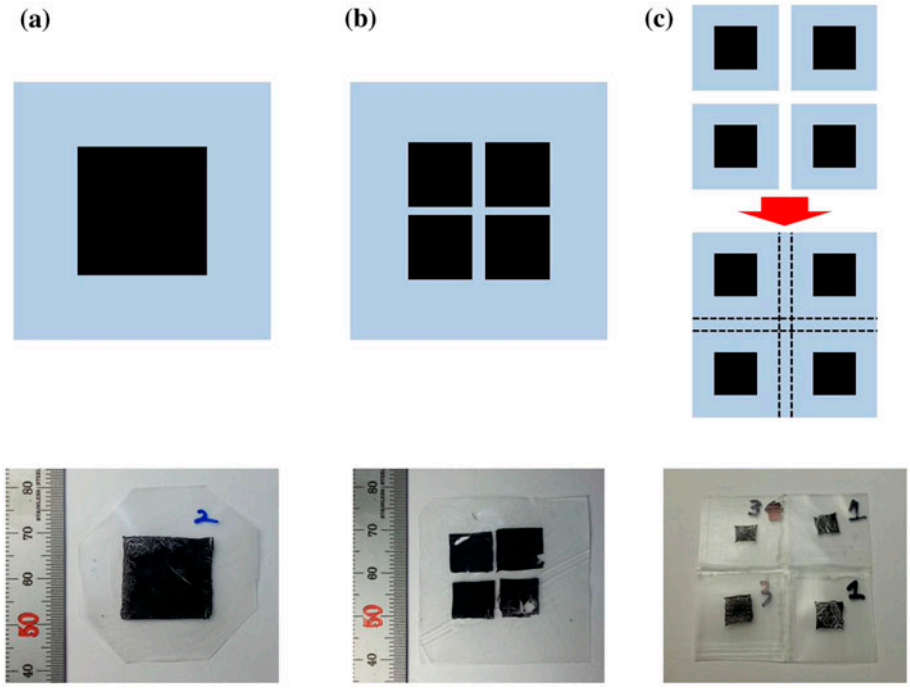

Fig. 4. Schematics of scale-up approaches for VA CNT membranes; (a) an enlarged VA CNT forest (2×2 cm^2), (b) sequential VA CNT forests (1×1 cm^2) in a large cast, and (c) a VA CNT membrane assembly.

3.2. Flux enhancement of VA CNT membrane

Fig. 3 presents the cross-sectional SEM images of a pristine VA CNT forest and a two times densified VA CNT forest. The two times densified VA CNT forest showed more CNTs within same magnification, indicating a higher pore density in the VA CNT membrane. This mechanical densification enhanced the membrane tortuosity. According to our previous study, the tortuosity was enhanced from 1.2 to 1.1 [19]. Table 1 shows the water permeability of a pristine VA CNT membrane and a two times densified VA CNT membrane. The membrane with the greater CNT density (1.3×10^{11}#/cm^2) displayed nearly twice the water permeability (2,070 LMH bar^{-1}). Interestingly, more than two times densified VA CNT membrane showed indication of a leak. This was likely due to the inability for epoxy resin to fully fill the CNT interstitial voids (data not shown). Furthermore, a two times densified VA CNT membrane showed 1,910 LMH bar^{-1} water permeability and no NaCl rejection when the desalination potential was evaluated.

3.3. Scale-up of the VA CNT membrane in laboratory scale

Fig. 4 shows the proposed scale-up approaches for VA CNT membranes. Three approaches are suggested: an enlarged VA CNT forest (2×2 cm^2; Fig. 4(a)), sequential VA CNT forests (1×1 cm^2) in a large cast (Fig. 4(b)), and a VA CNT membrane assembly (Fig. 4(c)). These scale-ups have some limitations. For example, an enlarged VA CNT forest is difficult to homogeneously produce. The other approaches require a large epoxy areas, i.e. the effective membrane area is inefficiently smaller than the actual membrane area.

4. Conclusion

VA CNT membranes have been used for high-performance water treatment. In this paper, we attempted to develop the desalination potential and increase the flux of VA CNT membranes and further proposed various scale-up approaches. Firstly, the desalination potential of the VA CNT membrane was evaluated by coating GO and PA as selective layers. The resultant membranes showed approximately 4–5 LMH bar^{-1} water permeability with 40–65% salt rejection. The water permeability of GO-coated VA CNT membrane were enhanced with a 0.01 M PAH coating, which prevented the GO layers from directly blocking water pathways. Second, water permeability was enhanced by the densification of the VA CNT forest, which resulted in increased pore density. Finally, three

scale-up approaches for VA CNT membranes were suggested. Further improvements to VA CNT membranes are required to apply in practical water treatment processes. These include characterizations of vertical alignment of CNT in the membrane, the ability to synthesize uniform CNTs with small pores, improved salt rejection with maintaining high water permeability and innovative scale-up methods.

Acknowledgments

This research was supported by the K-water Research & Business Project (K_RBP-1), a grant (15IFIP-B065893-03) from Industrial Facilities & Infrastructure Research Program funded by Ministry of Land, Infrastructure and Transport of Korean government, and the National Research Foundation of Korea Grant of the Korean Government (NRF-2010-C1AAA01-0029081).

Nomenclature

a_{c-c}	—	C–C bond length in a nanotube (nm)
A	—	effective area of the membrane (cm^2)
C_f	—	salt concentration of the feed (mg/L)
C_p	—	salt concentration of the permeate (mg/L)
d_{outer}	—	diameter of CNT outer-wall (nm)
J_w	—	water permeability (L m^{-2} h^{-1} (LMH) bar^{-1})
L	—	CNT height (cm)
m_c	—	mass of one carbon atom (mg)
M	—	mass of CNTs (mg)
N	—	average wall number (#)
R	—	rejection rate (%)
S	—	CNT growth area (cm^2)
t	—	measurement time (min)
V	—	volume of the collected permeate (mL)
Δ	—	difference operator

References

[1] S. Kar, R.C. Bindal, P.K. Tewari, Carbon nanotube membranes for desalination and water purification: Challenges and opportunities, Nano Today 7 (2012) 385–389.
[2] E. Drioli, L. Giorno, Comprehensive Membrane Science and Engineering, vol. 1, Elsevier Science, Amsterdam, 2010.
[3] A. Noy, H.G. Park, F. Fornasiero, J.K. Holt, C.P. Grigoropoulos, O. Bakajin, Nanofluidics in carbon nanotubes, Nano Today 2 (2007) 22–29.
[4] Q. Li, S. Mahendra, D.Y. Lyon, L. Brunet, M.V. Liga, D. Li, P. Alvarez, Antimicrobial nanomaterials for water disinfection and microbial control: Potential applications and implications, Water Res. 42 (2008) 4591–4602.
[5] C.H. Ahn, Y. Baek, C. Lee, S.O. Kim, S. Kim, S. Lee, S.-H. Kim, S.S. Bae, J. Park, J. Yoon, Carbon nanotube-based membranes: Fabrication and application to desalination, J. Ind. Eng. Chem. 18 (2012) 1551–1559.
[6] G. Hummer, J.C. Rasaiah, J.P. Noworyta, Water conduction through the hydrophobic channel of a carbon nanotube, Nature 414 (2001) 188–190.
[7] J.K. Holt, H.G. Park, Y. Wang, M. Stadermann, A.B. Artyukhin, C.P. Grigoropoulos, A. Noy, O. Bakajin, Fast mass transport through sub-2-nanometer carbon nanotubes, Science 312 (2006) 1034–1037.
[8] B.J. Hinds, N. Chopra, T. Rantell, R. Andrews, V. Gavalas, L.G. Bachas, Aligned multiwalled carbon nanotube membranes, Science 303 (2004) 62–65.
[9] Y. Baek, C. Kim, D.K. Seo, T. Kim, J.S. Lee, Y.H. Kim, K.H. Ahn, S.S. Bae, S.C. Lee, J. Lim, K. Lee, J. Yoon, High performance and antifouling vertically aligned carbon nanotube membrane for water purification, J. Membr. Sci. 460 (2014) 171–177.
[10] B. Corry, Designing carbon nanotube membranes for efficient water desalination, J. Phys. Chem. B 112 (2008) 1427–1434.
[11] F. Fornasiero, H.G. Park, J.K. Holt, M. Stadermann, C.P. Grigoropoulos, A. Noy, O. Bakajin, Ion exclusion by sub-2-nm carbon nanotube pores, Proc. Natl. Acad. Sci. 105 (2008) 17250–17255.
[12] M. Majumder, N. Chopra, B.J. Hinds, Effect of tip functionalization on transport through vertically oriented carbon nanotube membranes, J. Am. Chem. Soc. 127 (2005) 9062–9070.
[13] S.M. Park, J. Jung, S. Lee, Y. Baek, J. Yoon, D.K. Seo, Y.H. Kim, Fouling and rejection behavior of carbon nanotube membranes, Desalination 343 (2014) 180–186.
[14] S.P. Patole, P.S. Alegaonkar, H.-C. Shin, J.-B. Yoo, Alignment and wall control of ultra long carbon nanotubes in water assisted chemical vapour deposition, J. Phys. D Appl. Phys. 41 (2008) 155311-1–155311-6.
[15] S.P. Patole, P.S. Alegaonkar, H.-C. Lee, J.-B. Yoo, Optimization of water assisted chemical vapor deposition parameters for super growth of carbon nanotubes, Carbon 46 (2008) 1987–1993.
[16] D.C. Marcano, D.V. Kosynkin, J.M. Berlin, A. Sinitskii, Z. Sun, A. Slesarev, L.B. Alemany, W. Lu, J.M. Tour, Improved synthesis of graphene oxide, ACS Nano 4 (2010) 4806–4814.
[17] T.J. Kang, M. Cha, E.Y. Jang, J. Shin, H.U. Im, Y. Kim, J. Lee, Y.H. Kim, Ultra-thin and conductive nanomembrane arrays for nanomechanical transducers, Adv. Mater. 20 (2008) 3131–3137.
[18] H.J. Kim, K. Choi, Y. Baek, D.-G. Kim, J. Shim, J. Yoon, J.-C. Lee, High-performance reverse osmosis CNT/polyamide nanocomposite membrane by controlled interfacial interactions, ACS Appl. Mater. Interfaces 6 (2014) 2819–2829.
[19] B. Lee, Y. Baek, M. Lee, D.H. Jeong, H.H. Lee, J. Yoon, Y.H. Kim, A carbon nanotube wall membrane for water treatment, Nat. Commun. 6 (2015) 7109-1–7109-7.
[20] D.R. Dreyer, S. Park, C.W. Bielawski, R.S. Ruoff, The chemistry of graphene oxide, Chem. Soc. Rev. 39 (2010) 228–240.
[21] D. Yang, A. Velamakanni, G. Bozoklu, S. Park, M. Stoller, R.D. Piner, S. Stankovich, I. Jung, D.A. Field, C.A. Ventrice, Chemical analysis of graphene oxide

films after heat and chemical treatments by X-ray photoelectron and Micro–Raman spectroscopy, Carbon 47 (2009) 145–152.
[22] S.-Y. Kwak, S.G. Jung, S.H. Kim, Structure-motion-performance relationship of flux-enhanced reverse osmosis (ro) membranes composed of aromatic polyamide thin films, Environ. Sci. Technol. 35 (2001) 4334–4340.
[23] E.M.V. Hoek, S. Bhattacharjee, M. Elimelech, Effect of membrane surface roughness on colloid−membrane DLVO interactions, Langmuir 19 (2003) 4836–4847.
[24] Y. Han, Z. Xu, C. Gao, Ultrathin graphene nanofiltration membrane for water purification, Adv. Funct. Mater. 23 (2013) 3693–3700.
[25] M. Hu, B. Mi, Enabling graphene oxide nanosheets as water separation membranes, Environ. Sci. Technol. 47 (2013) 3715–3723.
[26] K. Goh, L. Setiawan, L. Wei, R. Si, A.G. Fane, R. Wang, Y. Chen, Graphene oxide as effective selective barriers on a hollow fiber membrane for water treatment process, J. Membr. Sci. 474 (2015) 244–253.
[27] D. Li, M.B. Müller, S. Gilje, R.B. Kaner, G.G. Wallace, Processable aqueous dispersions of graphene nanosheets, Nat. Nanotechnol. 3 (2008) 101–105.
[28] R.R. Nair, H.A. Wu, P.N. Jayaram, I.V. Grigorieva, A.K. Geim, Unimpeded permeation of water through helium-leak-tight graphene-based membranes, Science 335 (2012) 442–444.
[29] B.E. Conway, Ionic Hydration in Chemistry and Biophysics, vol. 12, Elsevier Science Ltd, New York, NY and Amsterdam, 1981.
[30] R.K. Joshi, P. Carbone, F.C. Wang, V.G. Kravets, Y. Su, I.V. Grigorieva, H.A. Wu, A.K. Geim, R.R. Nair, Precise and ultrafast molecular sieving through graphene oxide membranes, Science 343 (2014) 752–754.
[31] G.F. Zhong, T. Iwasaki, H. Kawarada, Semi-quantitative study on the fabrication of densely packed and vertically aligned single-walled carbon nanotubes, Carbon 44 (2006) 2009–2014.